

## N O T I C E

THIS DOCUMENT HAS BEEN REPRODUCED FROM  
MICROFICHE. ALTHOUGH IT IS RECOGNIZED THAT  
CERTAIN PORTIONS ARE ILLEGIBLE, IT IS BEING RELEASED  
IN THE INTEREST OF MAKING AVAILABLE AS MUCH  
INFORMATION AS POSSIBLE

NASA Technical Memorandum 81448

(NASA-TM-81448) EFFECTS OF FINE POROSITY ON  
THE FATIGUE BEHAVIOR OF A POWDER METALLURGY  
SUPERALLOY (NASA) 25 p HC A02/MF A01

N80-21493

CSCL 11F

Unclas

G3/26 47651

EFFECTS OF FINE POROSITY ON THE  
FATIGUE BEHAVIOR OF A POWDER  
METALLURGY SUPERALLOY

R. V. Miner and R. L. Dreshfield  
Lewis Research Center  
Cleveland, Ohio

Prepared for the  
Annual Meeting of the American Institute of Mining,  
Metallurgical and Petroleum Engineers  
Las Vegas, Nevada, February 24-28, 1980



EFFECTS OF FINE POROSITY ON THE FATIGUE BEHAVIOR  
OF A POWDER METALLURGY SUPERALLOY

by R. V. Miner and R. L. Dreshfield

National Aeronautics and Space Administration  
Lewis Research Center  
Cleveland, Ohio

ABSTRACT

E-367

Hot-isostatically-pressed powder-metallurgy Astroloy was obtained which contained 1.4 percent, fine porosity at the grain boundaries produced by argon entering the powder container during pressing. This material was tested at 650° C in fatigue, creep-fatigue, tension, and stress-rupture and the results compared with previous data on sound Astroloy. The pores averaged about 2 μm diameter and 20 μm spacing. They did influence fatigue crack initiation and produced a more intergranular mode of propagation. However, fatigue life was not drastically reduced. A large 25 μm pore in one specimen resulting from a hollow particle did reduce life by 60 percent, however. Fatigue behavior of the porous material showed typical correlation with tensile behavior. The plastic strain range-life relation was reduced proportionately with the reduction in tensile ductility, but the elastic strain range-life relation was little changed reflecting the small reduction in  $\sigma_u/E$  for the porous material.

INTRODUCTION

Production of components by powder metallurgy methods for critical applications in gas turbine engines such as disks and shafts is an important developing technology. It provides both material and cost savings and a greater uniformity of microstructure over parts forged from ingot. A need remains, however, to fully understand effects of the defects peculiar to

these powder metallurgy products which might limit achievement of their full potential, and also to develop improved production methods to minimize the frequency of these defects. The defects of chief concern are oxide inclusions and pores. Oxides can be present in the ingot starting material or produced by reaction or erosion of the ceramic parts of the atomization equipment in contact with the melt. Pores can also have several sources. A considerable amount of superalloy powder is produced by argon atomization and always handled in argon to prevent contamination. One possible source of pores are hollow powder particles filled with argon that are occasionally produced in the atomization process. A second possible source of porosity is the lack of complete evacuation of the argon cover gas from the powder container before consolidation. This study is concerned with the effects of porosity from still another source.

In this case a small leak in the powder container allowed some argon, the pressurizing medium used in hot-isostatic-pressing, to be pumped in and entrapped in the part which did not fully consolidate, nevertheless. The part was to be a turbine disk of the nickel-base superalloy Astroloy made as part of a component demonstration program.<sup>2</sup> The material taken for this study contained about 1.4 percent of fine grain boundary porosity with average pore diameter and spacing of about 2 and 20  $\mu\text{m}$ , respectively. The amount of porosity in this material exceeded the turbine engine manufacturer's specifications by roughly 15 times. Still, it was of interest to determine the effect of such a fine, but abundant porosity on critical mechanical properties, particularly low cycle fatigue behavior since turbine disk life is limited by fatigue. This work is part of a larger investigation which also included a more extensive evaluation of tensile and stress-rupture behavior.<sup>3</sup>

It is stressed that this work does not establish the minimum property levels controlled by whatever large but rare defects this material may contain. Such determinations require testing of a large volume of material. In general, failure in the tests to be reported was associated with the fine general grain boundary porosity, not an isolated large pore or cluster of pores.

Fatigue and creep-fatigue tests were conducted on the porous Astroloy at 650° C and a variety of strain ranges. Comparable data on sound Astroloy already existed.<sup>4</sup> The failed specimens of both the porous and sound materials were examined by scanning electron microscopy to determine the type and size of defect, if any, which initiated failure for possible correlation with the life of the specimen. Modes of crack initiation and propagation were also noted. Tensile and stress-rupture properties at 650° C were measured for both materials also.

## MATERIALS AND PROCEDURES

### Materials

The material studied in this program was hot-isostatically-pressed, powder-metallurgy, low-carbon Astroloy. Both the sound and porous materials were taken from full scale pressings for an aircraft engine first stage turbine disk. Both were produced according to the engine manufacturer's specifications but at different times. The processing methods employed are fully described elsewhere<sup>2</sup> and will be only briefly discussed here.

Composition specifications for low carbon Astroloy and the compositions of the sound and porous pressings are presented in Table I. The compositions of both pressings meet the specifications and are very nearly the same. Both materials were produced from -80 mesh powder from the same manu-

facturer. The powder was loaded into mild steel containers shaped like the part, hot outgassed, sealed, and hot isostatically pressed for 3 hours at 100 MPa and 1190<sup>0</sup> or 1215<sup>0</sup> C for the sound or porous pressings, respectively. The pressings were solution treated at about 1110<sup>0</sup> C for 3 and 2 hours, respectively, for the sound and porous pressings. The hot isostatic pressing cycles and solution treatments for both pressings are within the manufacturer's range of specifications. Both were aged as follows: 870<sup>0</sup> C/8 hr/AC + 980<sup>0</sup> C/4 hr/AC + 650<sup>0</sup> C/24 hr/AC + 760<sup>0</sup> C/8 hr/AC.

As a part of the qualification testing for powder metallurgy Astroloy parts, a sample is subjected to 1205<sup>0</sup> C for 4 hours and then examined metallographically. This heating to just below the solidus causes any Ar in the material to produce visible voids. The porous pressing tested here failed this quality control test whereas the sound material passed. Just the 1110<sup>0</sup> C solution treatment was sufficient to produce the 1.4 percent of porosity observed in the portion of the pressing tested here.

#### Mechanical Testing

Strain-controlled, fully-reversed (ratio of minimum to maximum strain, R, equal to -1) low cycle fatigue tests were conducted at 0.33 Hz. Creep-fatigue tests were identically conducted except for a 15 minute tensile dwell at the maximum tensile strain of the cycle. Loading and unloading rates were constant and of equal magnitude and the same for both types of tests. The specimen finish, produced by fine grinding, was 0.2  $\mu\text{m}$  RMS. A complete description of the test methods and the results on the sound Astroloy have been previously presented.<sup>4</sup> Tensile and stress-rupture tests were conducted in accordance with ASTM recommended practice.

## RESULTS

### Microstructure

The microstructures of the sound and porous Astroloy pieces are shown in Fig. 1. The porous material contains about 1.4 percent porosity, most of it appearing at grain boundaries. The average pore size average lineal intercept, is 2  $\mu\text{m}$ , though some as large as 10  $\mu\text{m}$  were occasionally seen in metallographic specimens. The average spacing between the pores is about 20  $\mu\text{m}$ .

The average grain size of the porous material was 90  $\mu\text{m}$ , average lineal intercept. The grain size of the sound material was smaller, 50  $\mu\text{m}$ . The reason for this difference was apparently the difference in the hot-isotatic-pressing temperature. The porous material was compacted at 1215<sup>0</sup> C and the sound at 1190<sup>0</sup> C.

### Tensile and Stress-Rupture Behavior at 650<sup>0</sup> C

Average values of the 650<sup>0</sup> C tensile properties for the sound and porous materials and the percentage reductions for the porous material relative to the sound are presented in Table II. Results are the average of two tests. Data for the sound material is taken from Ref. 3. Also presented for future discussion are the values of the 650<sup>0</sup> C elastic modulus, ultimate tensile strength divided by modulus, and true tensile ductility. The modulus values are taken from the cyclic tests. They are the averages of the values from all the fatigue and creep-fatigue tests.

Note that the tensile strength of the porous material is a little reduced but its ductility is reduced substantially. Ultimate tensile strength is reduced 7 percent, but true tensile reduction of area ( $D_p$ ) is reduced about 40 percent. The elastic modulus of the porous material is also re-

duced such that ultimate strength divided by modulus is only reduced 1.5 percent relative to the sound material.

The 650° C stress-rupture data obtained has been analyzed to obtain approximate stresses for 10, 100, and 1000 hours life. These values are reported in Table II for both materials together with the percentage reductions for the porous material relative to the sound. Rupture ductility for both materials was roughly independent of time to failure for the same range of lives and an average value has been reported for each material.

The reduction in stress rupture strength for the porous material is small, about 5 percent for 100 hours life, and only 2 percent for 1000 hours life. True stress-rupture reduction of area ( $D_c$ ) for the porous material is more reduced, about 20 percent, but not as much as was the 650° C true tensile ductility.

#### Low Cycle Fatigue and Creep-Fatigue Behavior

Strain-controlled low cycle fatigue tests and creep-fatigue tests incorporating a 15 minute dwell at maximum tensile strain were conducted at 650° C and  $R = -1$  for a variety of strain ranges. The data are presented in Table III. Shown are the total ( $\Delta\epsilon_t$ ), elastic ( $\Delta\epsilon_e$ ), inelastic ( $\Delta\epsilon_{in}$ ), and creep ( $\Delta\epsilon_c$ ) strain range components, the stress range at the first cycle ( $N_1$ ) and at half life ( $N_{f/2}$ ), the mean stress at half life, the number of cycles to 5 percent load drop ( $N_5$ ), and the number of cycles to failure ( $N_f$ ). The creep strain,  $\Delta\epsilon_c$ , is defined as the stress relaxation occurring during the tensile dwell divided by the modulus, and  $\Delta\epsilon_{in}$  is the sum of  $\Delta\epsilon_c$  and  $\Delta\epsilon_p$ , the plastic strain range. The elastic strain range has been calculated from the maximum stress range less any creep relaxation and the average value of the modulus for the material from all the tests.

From the values of the stress range at  $N_1$  and  $N_f/2$  it can be seen that both materials were cyclically stable under both cycles except at the highest strain ranges. In fatigue at  $\Delta\epsilon_t \cong 0.014$ , the porous material cyclically hardened slightly, about 3 percent, but the sound material did not cyclically harden except at the highest strain range,  $\Delta\epsilon_t \cong 0.019$ , where it hardened about 7 percent. Both materials cyclically hardened slightly at the highest strain ranges in the creep-fatigue cycle, about 3 percent. Slightly negative mean stresses developed in most of the tests but all were less than 5 percent of the stress range.

The cyclic stress-strain behavior of both materials under both cycles is shown in Fig. 2. The stabilized stress range was taken as that at half life. The line shown represents the equation  $\Delta\sigma = 3540 \Delta\epsilon_p^{0.097}$  which was obtained by fitting all of the fatigue data for both materials for  $\Delta\epsilon_p \geq 10^{-4}$ . It can be seen that both materials exhibit very similar behavior under both cycles. The creep-fatigue data also fit this line at the higher strain ranges, however, at the lower strain ranges it appears that the stress range may be smaller for the creep-fatigue cycle.

The relationship between  $\Delta\epsilon_{in}$  and  $N_f$  for both materials and cycles is shown in Fig. 3. For the fatigue tests on the porous material at the lowest  $\Delta\epsilon_t$ ,  $\Delta\epsilon_{in}$  is uncertain since it was less than the detectable limit of about  $5 \times 10^{-5}$ . Lacking these points, a line has been drawn through the points at the higher  $\Delta\epsilon_{in}$  assuming a slope equal to that for the sound material just to provide easier visual comparison. Regardless of this device, it can be seen that the inelastic strain range capability of the porous material is about 40 percent lower than that of the sound material for both cycles.

The relationship between  $\Delta\epsilon_e$  and  $N_f$  for each cycle is very nearly the same for both materials, and is very nearly the same as that between  $\Delta\epsilon_t$  and  $N_f$ , since  $\Delta\epsilon_{in}$  is so small compared to  $\Delta\epsilon_e$  in these tests. The relationship between  $\Delta\epsilon_t$  and  $N_f$  is shown in Fig. 4. The lines represent the sum of regression fit equations for  $\Delta\epsilon_{in}$  and  $\Delta\epsilon_e$  of the form  $\Delta\epsilon = aN_f^b$ , except for the sound material tested in fatigue where an equation of the form  $\Delta\epsilon_e = aN_f^b + c$  was found to provide a better fit.

The fine porosity does not have as great an effect on fatigue and creep-fatigue behavior as might have been feared. Reductions in life relative to those for the sound material are about 30 percent for both test cycles.

#### Fractography

All of the failed specimens of both materials from the fatigue and creep-fatigue tests were examined by scanning electron microscopy as well as selected tensile and stress-rupture specimens.

Tensile and stress-rupture. - Tensile failure in the sound material at 650° C was transgranular with a ductile, dimpled appearance. Failure in the porous material changed to intergranular. The corresponding reduction in tensile ductility was 40 percent. Stress-rupture failure was intergranular in both materials, however, and the ductility of the porous material was reduced only 20 percent relative to that of the sound material.

Fatigue. - In the sound material, the fatigue cycle produced multiple surface crack initiation in a transgranular mode at all strain ranges. The appearances of two specimens tested at the lower strain ranges shown in Fig. 5 typify the initiation sites. Crack initiation has occurred on a machining mark at what appears to be a grain boundary. Stereographic exami-

nation shows the particle near the origin in Fig. 5(a) to be an artifact sitting on the edge of the specimen. In the area immediately around the origin is a relatively featureless Stage II type of transgranular fracture. Beyond this area in the specimen tested at the lower strain range, Fig. 5(a), there is an area roughly five grains deep that has some crystallographic character. Beyond that is an area of rougher Stage II propagation. Fracture on the specimen tested at the higher strain range, Fig. 5(b) goes from the smooth to rougher Stage II appearance directly.

Failure in the two specimens of the porous material tested at the low strain ranges,  $\Delta\epsilon_t \cong 0.008$ , clearly initiated at pores. Unlike the sound material, failure initiated at single sites. The specimen shown in Fig. 6(a) failed in the area of two closely spaced pores about 5  $\mu\text{m}$  in diameter. The larger particles near the pores are artifacts sitting on the surface. The area near the pores appears like Stage I crystallographic fracture. Striations on Stage I fracture faces do occur in Ni-base superalloys.<sup>5</sup> This flat crystallographic appearance was not observed on other specimens, and even in this case the crack propagation mode quickly changed to a rough Stage II appearance.

These 5  $\mu\text{m}$  pores produced no significant reduction in life relative to that expected for the sound material. The data point representing this test falls on the curve of  $\Delta\epsilon_t$  vs  $N_f$  representing the sound material (Fig. 4).

The second specimen of the porous material, Fig. 6(b), failed at a large 25  $\mu\text{m}$  diameter pore. This pore is probably not part of the general fine porosity caused by the leaking container during hot-isostatic-pressing. Its surface appears to have the solidification structure seen inside hollow pow-

der particles. Crack propagation from this large pore has immediately assumed a rough Stage II mode. The life of this specimen was reduced about 60 percent relative to that expected for the sound material at the same  $\Delta\epsilon_t$  and has largely contributed to the 30 percent reduction in average behavior for the porous material.

Crack propagation in the sound material except at the highest strain range maintained a rough Stage II appearance until overload failure occurred. In the porous material, however, once the crack progressed a few hundred  $\mu\text{m}$ , the propagation mode became partially intergranular. At the highest strain ranges,  $\Delta\epsilon_t \cong 0.014$ , fracture in the porous material was almost entirely intergranular. The specimen tested at  $\Delta\epsilon_t = 0.0138$  appeared to have fractured entirely intergranularly. However, the specimen tested at  $\Delta\epsilon_t = 0.135$ , Fig. 7, appears to have a small area of transgranular fracture. Many secondary cracks were observed on both specimens.

In the sound material at the highest strain range employed,  $\Delta\epsilon_t = 0.0191$ , fracture remained transgranular though it became very rough. There was no region of smooth Stage II fracture as for the lower strain ranges.

The fatigue behavior of Udimet 700, an alloy very similar to the Astroloy studied here except primarily for a higher C concentration, 0.06 w/o, and a larger grain size, about 200  $\mu\text{m}$ , has been studied extensively. Wells and Sullivan<sup>6</sup> tested Udimet 700 at the same temperature employed here, 650<sup>o</sup> C, with  $\Delta\epsilon_t = 0.016$ . However, there were significant differences. They employed a strain ratio of 0, a lower frequency of the order of 0.01 Hz, and highly polished specimens. Fracture initiation was as often transgranular Stage I as it was intergranular. Though even when crack ini-

tiation was intergranular, the propagation mode changed to Stage I at about one grain diameter below the surface. The difference in fracture initiation behavior observed here is easily explained by the fine ground, 0.2  $\mu\text{m}$  RMS surface on the specimens tested here. However, the frequent lack of any Stage I fracture area on the Astroloy specimens tested here is not understood. The higher frequency employed here would be expected to promote Stage I fracture.<sup>7</sup>

Creep-fatigue cycle. - During the creep-fatigue cycle which incorporated a 15 minute dwell at the maximum strain both the sound and porous materials cracked intergranularly at all the strain ranges tested. On the gage surface of the tested specimens, many grain boundaries could be seen to have opened. Generally, crack initiation sites could not be precisely distinguished because there was no Stage I or smooth Stage II area to mark them.

#### DISCUSSION

Many examples exist of drastic reductions in ductility produced by small amounts of porosity concentrated on grain boundaries in metals. The case of voids produced by irradiation generated helium closely represents that of the argon containing voids discussed here. Helium concentrations of a few ppm commonly reduce elevated temperature tensile ductility from 50 to 80 percent, though a few alloys are relatively unaffected.<sup>8</sup> The 700° C tensile ductility of Inconel X-750, a superalloy containing about 15 percent  $\gamma'$ , was reduced 75 percent by 7 ppm He. A helium concentration of only 0.4 ppm reduced the creep ductility of Ni-6 $\Delta$ W about an order of magnitude.<sup>9</sup> Voids produced upon heating after 15 percent tensile prestraining reduced the 750° C creep ductility of the superalloy Nimonic 80A by 80 to 90 percent.<sup>10</sup>

Generally, the cavities shown in the cases of large ductility reductions cited are of the order of  $0.5 \mu\text{m}$  in diameter and a few  $\mu\text{m}$  apart along the grain boundaries. Models by Nix, Matlock, and DiMelfi<sup>11</sup> and by Pavinich and Raj<sup>12</sup> of the effect of grain boundary cavities growing by creep on rupture life and ductility show that the spacing between the cavities is most important rather than simply the amount of porosity. In order for cavities to interact and cause large reductions in ductility, the spacing between them must be small enough for localization of strain in the material between the pores leading to grain boundary failure at low overall strains. To apply these models additional information is required such as the creep strain rate sensitivity and contribution of grain boundary sliding to the total strain. However, qualitatively the relatively small effect of the porosity observed here on the stress rupture ductility of Astroloy can be understood. Though a considerable amount of porosity is present, 1.4 percent, the pores are too large and widely spaced along the grain boundaries to interact strongly.

On the other hand, the typical pores in this material are too small, less than  $10 \mu\text{m}$ , to greatly reduce the number of cycles required to initiate a fatigue crack in this material. To see this most clearly we should look at the tests of the lowest strain ranges where relatively more of the life should be spent in crack initiation than for tests at the higher strain ranges. The porous specimen cycled at  $\Delta\epsilon_t = 0.0079$  shown in Fig. 6(a) failed from two closely spaced pores about  $5 \mu\text{m}$  in diameter but had a life not significantly different from that expected for the sound material. A considerably larger pore such as the  $25 \mu\text{m}$  diameter pore in the specimen cycled at  $\Delta\epsilon_t = 0.0077$  shown in Fig. 6(b) is necessary to produce a

significant reduction in the life to crack initiation. That specimen failed at about half the life expected for the sound material.

The mode of fatigue crack propagation was affected by the porosity, becoming more intergranular in the porous material than in the sound material. Still, at the higher strain ranges  $\Delta\epsilon_t \cong 0.014$ , where the mode of crack propagation was most different in the two materials, the difference in total life was only about 30 percent, some of which may be due to earlier crack initiation in the porous material.

The simplest way to view the fatigue behavior of the porous Astroloy is just as Astroloy of lower ductility. The differences in fatigue behavior are what would be expected based on the tensile properties of the two materials using the usual rules of thumb.<sup>13</sup> That is, there is little difference between the elastic strain range vs. life relations for the two materials, since typically  $\Delta\epsilon_e \propto \sigma_u/E N_f^{-b}$ , where  $b$  is a constant, and  $\sigma_u/E$  is nearly the same for both materials. There is, however, as should be expected, a difference in the plastic strain range vs. life relationship between the two materials. Typically for high temperature materials,  $\Delta\epsilon_p = 0.5 D_p N_f^{-d}$ , where  $D_p$  is the true tensile reduction of area and  $d$  is a constant.<sup>14</sup> The ratio between the two materials of the  $\Delta\epsilon_p$  for a given life, Fig. 3, is very nearly that for their true tensile ductilities, Table II.

#### SUMMARY OF FINDINGS

Hot-isostatically-pressed powder-metallurgy Astroloy containing about 1.4 percent of fine grain boundary porosity produced by argon entering the powder container during pressing was studied in this investigation. The pores had a 2  $\mu\text{m}$  average diameter and 20  $\mu\text{m}$  spacing. This material was

tested in fatigue at 650<sup>0</sup> C and  $R = -1$  at various strain ranges and in creep-fatigue by incorporating a 15 minute dwell in the cycle. Tensile and stress-rupture tests were also performed. These results are compared with those obtained previously on sound Astroloy.

1. In comparison with the sound material, 650<sup>0</sup> C tensile and stress-rupture strengths of the porous material were reduced less than 7 percent. Strength divided by modulus was nearly unchanged.

2. Tensile ductility of the porous material was reduced 40 percent and was associated with a change from transgranular failure in the sound material to intergranular in the porous. Stress-rupture failure was intergranular in both materials and ductility was reduced 20 percent in the porous material.

3. Fatigue behavior showed typical correlation with tensile behavior. The plastic strain range-life relation was reduced proportionately with reduction in tensile ductility and the elastic strain range - life relation was little affected reflecting the small difference in  $\sigma_u/E$  for the two materials.

4. At low strain ranges,  $\Delta\epsilon_t \cong 0.008$ , fatigue failure in the porous material initiated at pores. Initiation at small pores, about 5  $\mu\text{m}$  diameter, did not greatly reduce life. However, the life of one specimen was reduced 60 percent by a large 25  $\mu\text{m}$  pore resulting from a hollow powder particle.

5. Fatigue failure became more intergranular in the porous material at  $\Delta\epsilon_t \cong 0.014$  than in the sound material, though the reduction in life was about the same as at the lower  $\Delta\epsilon_t$ , 30 percent.

6. Creep-fatigue life was about 30 percent lower for the porous material than for the sound material. Failure was completely intergranular in both materials.

#### REFERENCES

1. D. Eylon and J. M. Hyzak: Metall. Trans., 1978, vol. 9A, pp. 127-129.
2. R. D. Eng and D. J. Evans: Report No. PWA-5574-12-VOL-1, Pratt & Whitney Aircraft Group, East Hartford, CT, March 1978. (NASA CR-135409.)
3. R. L. Dreshfield and R. V. Miner, Jr.: Report No. NASA TM X-79263, National Aeronautics and Space Administration, Washington, D.C., 1979.
4. B. A. Cowles, D. L. Sims, J. R. Warren and R. V. Miner, Jr.: Evaluation of the Cyclic Behavior of Aircraft Turbine Disk Alloys, J. Eng. Matls. and Tech., to be published.
5. M. Gell and G. R. Leverant: Acta Metall., 1968, vol. 16, pp. 553-561.
6. C. H. Wells and C. P. Sullivan: ASM Trans., 1967, vol. 60, pp. 217-222.
7. F. E. Organ and M. Gell: Metall. Trans., 1971, vol. 2, pp. 943-952.
8. D. Kramer, K. R. Garr, A. G. Pard and C. G. Rhodes: AI-AEC-13047, Atomic Energy Commission, Washington, DC, 1972.
9. D. K. Matlock and W. D. Nix: J. Nucl. Mater., 1975, vol. 56, pp. 45-152.
10. B. F. Dyson and M. J. Rodgers: Met. Sci., 1974, vol. 8, pp. 261-266.
11. W. D. Nix, D. K. Matlock and R. J. DiMelfi: Acta Metall., 1977, vol. 25, pp. 495-503.
12. W. Pavinich and R. Raj: Metall. Trans., 1977, vol. 8A, pp. 1917-1933.
13. S. S. Manson: Exp. Mech., 1965, vol. 5, pp. 93-226.
14. G. R. Halford, J. F. Saltsman and M. H. Hirschberg: NASA TM-73737, National Aeronautics and Space Administration, Washington, DC, 1977.

TABLE I. - CHEMICAL SPECIFICATION FOR LOW CARBON ASTROLOY

Element	Aim, weight % (except as noted)		Actual, weight % (except as noted)	
	Min	Max	Porous	Sound
Carbon	0.02	0.04	0.024	0.023
Manganese	-----	.15	.001	.001
Silicon	-----	.20	.018	.06
Phosphorous	-----	.015	.005	<.005
Sulfur	-----	.015	.006	.003
Chromium	14.00	16.00	14.4	15.1
Cobalt	16.00	18.00	17.0	17.0
Molybdenum	4.50	5.50	5.3	5.2
Titanium	3.35	3.65	3.6	3.5
Aluminum	3.85	4.15	4.1	4.0
Boron	.015	.025	.021	.024
Zirconium	-----	.06	.002	<.01
Tungsten	-----	.05	.029	<.05
Iron	-----	.50	.09	.09
Copper	-----	.10	.05	<.05
Lead	-----	0.0010 (10 ppm)	<1 ppm	<1
Bismuth	-----	.00005 (0.5 ppm)	<0.2 ppm	<.3
Oxygen	-----	.010 (100 ppm)	90 ppm	80
Nitrogen	-----	.0050 (50 ppm)	6 ppm	23
Nickel	remainder			

TABLE II. - TENSILE AND STRESS-RUPTURE PROPERTIES OF SOUND AND POROUS ASTROLOY AT 650° C

650° C Tensile properties							
	0.2% yield strength, $\sigma_y$ , MPa	Ultimate tensile $\sigma_u$ , MPa	Elastic modulus, E, MPax10 <sup>-5</sup>	$\sigma_u/E$	Elongation, %	Reduction of area, %	True reduction of area, $D_p$
Sound Astroloy	880	1230	1.77	0.00695	30	36	0.46
Porous Astroloy	800	1150	1.68	.00685	25	25	.28
Reduction, %	9	7	5	1.5	18	33	.38
650° C Stress-rupture properties							
	Stress, 10 hr, MPa	Stress, 100 hr, MPa	Stress, 1000 hr, MPa	Average ductilities for 10 to 1000 hours life			
				Elongation, %	Reduction of area, %	True reduction of area, $D_c$	
Sound Astroloy	1010	910	760	15	19	0.21	
Porous Astroloy	940	860	745	13	16	.17	
Reduction, %	7	5	2	13	16	.19	

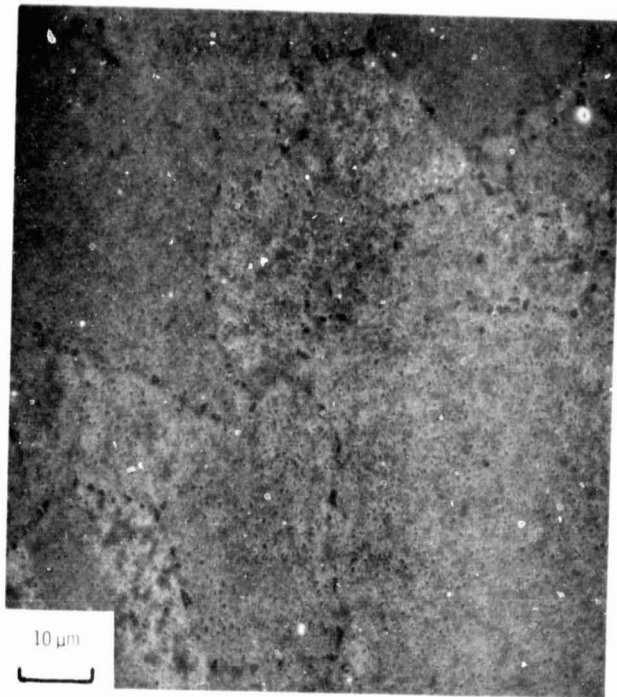
TABLE III. - FATIGUE AND CREEP-FATIGUE DATA ON SOUND AND POROUS ASTROLOY, 650° C, R = -1. FATIGUE TESTS WERE CONDUCTED AT 0.33 Hz. CREEP-FATIGUE TESTS INCORPORATED A 15 TENSILE DWELL AT MAXIMUM STRAIN

Material	Test	Specimen	Strain range				Stress range, $\Delta\sigma$ , MPa		Mean stress at $N_f/2$ , $\sigma$ , MPa	Cycles to failure	
			Total, $\Delta\epsilon_t$	Elastic, $\Delta\epsilon_e$	Inelastic, $\Delta\epsilon_{in}$	Creep, $\Delta\epsilon_c$	$^bN_1$	$N_f/2$		$N_5$	$N_f$
Sound	Fatigue	CB-16	0.0191	0.0133	0.0058	0	2170	2321	-28	248	261
		DB-1	.0140	.0109	.0032	↓	1910	1920	-56	850	961
		DB-2	.0099	.0095	.0004		1688	1674	-12	3,800	4,025
		DB-7	.0098	.0094	.0004		1708	1660	-19	2,900	3,121
		DB-4	.0085	.0084	.0001		1497	1478	-12	5,110	8,498
		DB-5	.0084	.0083	.0001		1476	1466	0	8,176	8,901
		DB-3	.0066	.0066	<.00005		1228	1170	0	-----	<sup>a</sup> 220,704
	Creep-fatigue	DB-10	0.0119	0.0108	0.0015		0.0006	1921	1943	-30	300
		DB-11	.0117	.0102	.0015	.0004	1855	1871	-50	605	697
		DB-13	.0078	.0077	.0001	.0001	1417	1375	0	7,420	7,780
		DB-12	.0079	.0076	.0003	.0001	1328	1355	-22	11,625	11,942
Porous	Fatigue	2	0.0138	0.0116	0.0020	0	1878	1942	-39	506	519
		1	.0135	.0115	.0020	↓	1852	1930	-37	601	670
		3	.0079	.0079	<.00005		1320	1320	-7	12,757	14,180
		4	.0077	.0077	<.00005		1304	1290	-27	9,067	9,605
	Creep-fatigue	5	0.0130	0.0110	0.0020		0.0004	1850	1905	-56	273
		6	.0112	.0102	.0010	.0002	1764	1750	-48	464	511
		8	.0111	.0100	.0011	.0002	1693	1713	-50	348	370
		7	.0080	.0079	.0001	<.00005	1348	1325	-60	8,782	8,860
		9	.0079	.0077	.0002	<.00005	1308	1297	-22	3,807	3,983

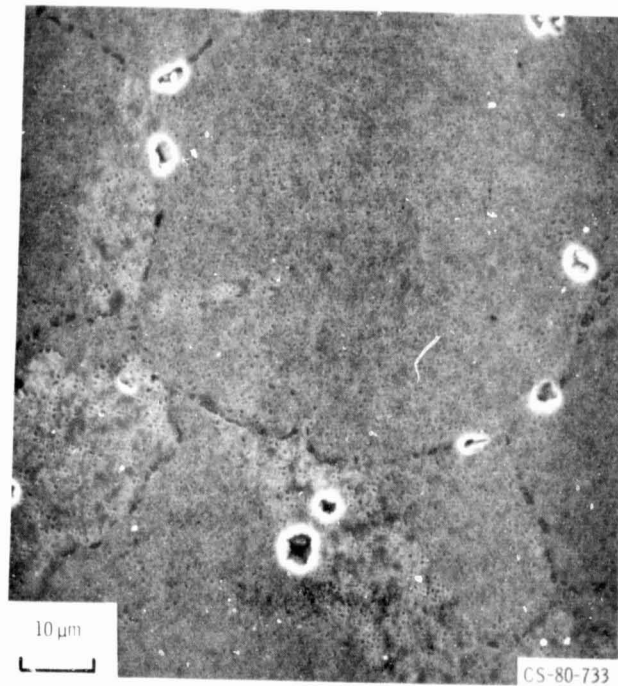
<sup>a</sup>Test discontinued.

<sup>b</sup> $N_1$  (first cycle),  $N_f/2$  (half life),  $N_5$  (life to 5% load drop),  $N_f$  (total separation).

ORIGINAL PAGE IS  
OF POOR QUALITY



(a) SOUND ASTROLOY.



(b) POROUS ASTROLOY.

Figure 1. - Microstructures of the sound and porous Astroloy.

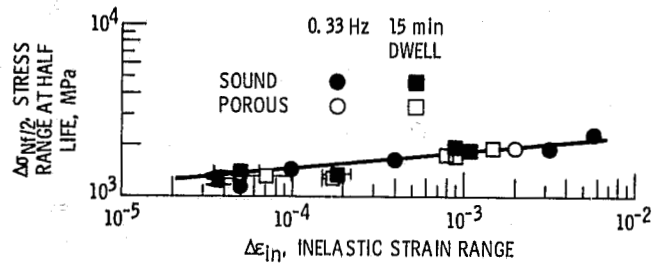


Figure 2. - Cyclic stress-strain behavior of sound and porous Astroloy at 650° C, R = -1.

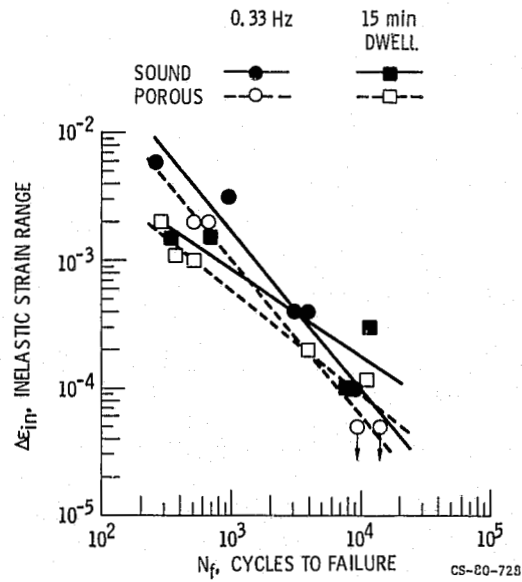


Figure 3. - Inelastic strain range versus life relations for sound and porous Astroloy, 650° C, R = -1.

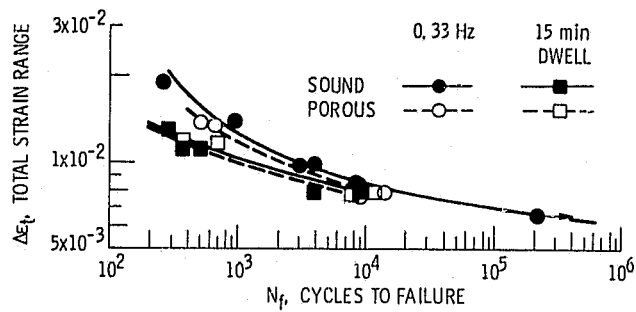
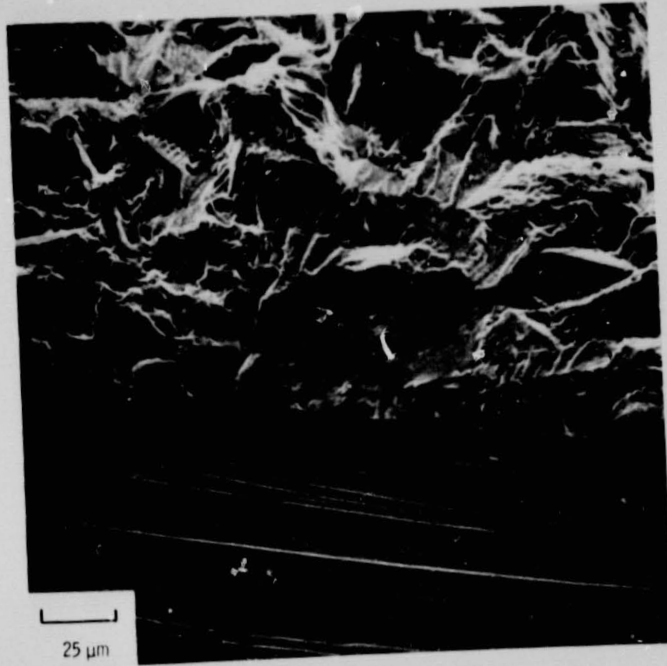
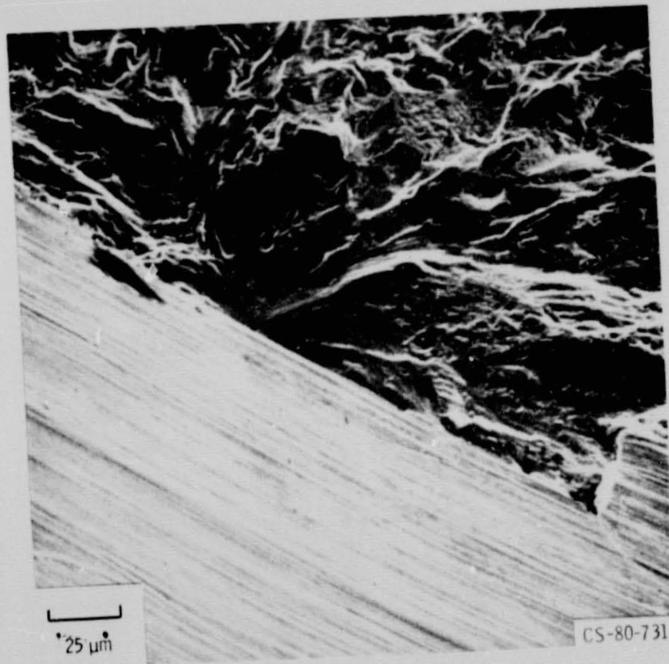


Figure 4. - Total strain range versus life relationship for porous and sound Astroloy, 650° C, R = -1.

ORIGINAL PAGE IS  
OF POOR QUALITY



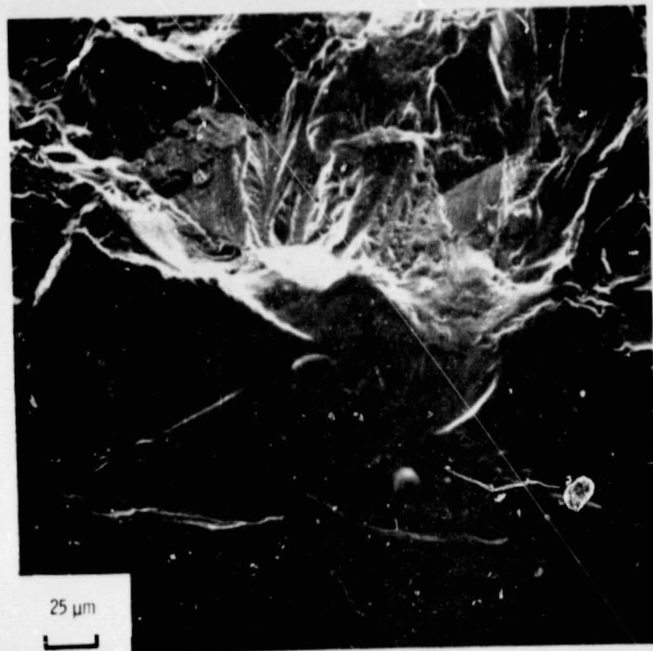
(a)  $\Delta\epsilon_f = 0.0085$ ,  $N_f = 8498$ .



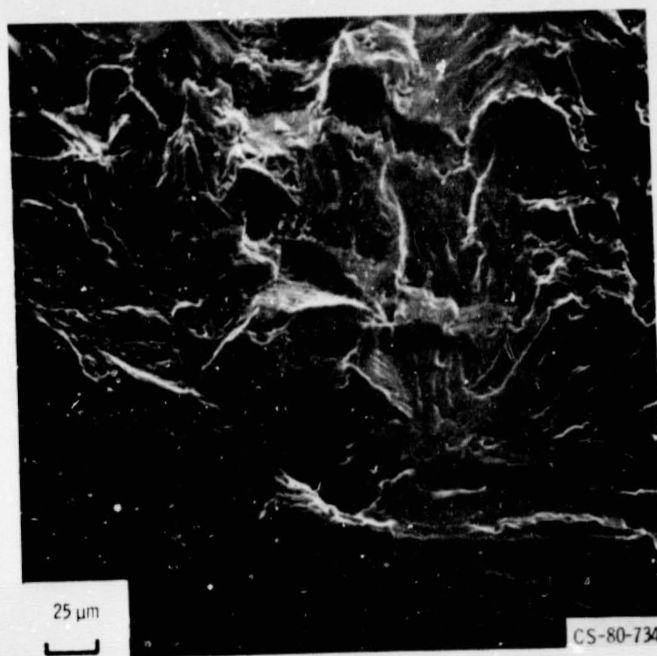
(b)  $\Delta\epsilon_f = 0.0098$ ,  $N_f = 4025$ .

Figure 5. - Fatigue failure initiation sites in sound Astroloy, 650° C, R = -1.

ORIGINAL PAGE IS  
OF POOR QUALITY



(a)  $\Delta\epsilon_f = 0.0079$ ,  $N_f = 14\ 180$ .



(b)  $\Delta\epsilon_f = 0.0077$ ,  $N_f = 9605$ .

Figure 6. Fatigue failure initiation sites in porous Astroloy, 650° C, R = -1.

ORIGINAL PAGE IS  
OF POOR QUALITY

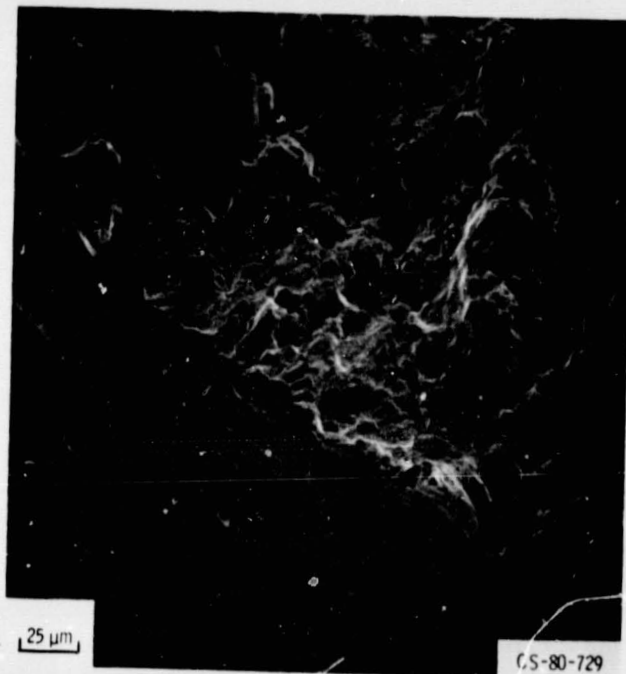


Figure 7. - Fatigue failure initiation site in porous Astroloy, 650° C, R = -1,  
 $\Delta\epsilon_f = 0.0135$ ,  $N_f = 670$ .

1. Report No. NASA TM-81448	2. Government Accession No.	3. Recipient's Catalog No.	
4. Title and Subtitle EFFECTS OF FINE POROSITY ON THE FATIGUE BEHAVIOR OF A POWDER METALLURGY SUPERALLOY		5. Report Date	
		6. Performing Organization Code	
7. Author(s) R. V. Miner and R. L. Dreshfield		8. Performing Organization Report No. E-367	
		10. Work Unit No.	
9. Performing Organization Name and Address National Aeronautics and Space Administration Lewis Research Center Cleveland, Ohio 44135		11. Contract or Grant No.	
		13. Type of Report and Period Covered Technical Memorandum	
12. Sponsoring Agency Name and Address National Aeronautics and Space Administration Washington, D. C. 20546		14. Sponsoring Agency Code	
		15. Supplementary Notes	
16. Abstract Hot-isostatically-pressed powder-metallurgy Astroloy was obtained which contained 1.4 percent fine porosity at the grain boundaries produced by argon entering the powder container during pressing. This material was tested at 650° C in fatigue, creep-fatigue, tension, and stress-rupture and the results compared with previous data on sound Astroloy. The pores averaged about 2 μm diameter and 20 μm spacing. They did influence fatigue crack initiation and produced a more intergranular mode of propagation. However, fatigue life was not drastically reduced. A large 25 μm pore in one specimen resulting from a hollow particle did reduce life by 60 percent, however. Fatigue behavior of the porous material showed typical correlation with tensile behavior. The plastic strain range-life relation was reduced proportionately with the reduction in tensile ductility, but the elastic strain range-life relation was little changed reflecting the small reduction in $\sigma_u/E$ for the porous material.			
17. Key Words (Suggested by Author(s)) Superalloys Powder metals Defects Fatigue		18. Distribution Statement Unclassified - unlimited STAR Category 26	
19. Security Classif. (of this report) Unclassified	20. Security Classif. (of this page) Unclassified	21. No. of Pages	22. Price*

\* For sale by the National Technical Information Service, Springfield, Virginia 22161